JOURNAL OF CATALYSIS 126, 519–531 (1990)

Methanol Adsorption and Decomposition on (1 × 1)Pt(110) and (2 × 1)Pt(110): Identification of the Active Site for Carbon–Oxygen Bond Scission during Alcohol Decomposition on Platinum

JIANHUA WANG AND R. I. MASEL[1]

University of Illinois, 1209 West California Street, Urbana, Illinois 61801

Received March 16, 1990; revised June 21, 1990

The adsorption and decomposition of methanol are examined on (1 × 1)Pt(110) and (2 × 1)Pt(110). It was found that (1 × 1)Pt(110) and (2 × 1)Pt(110) behave very differently even though they have a very similar surface structure. When methanol decomposes on (2 × 1)Pt(110) only CO and H_2 are formed. However, when methanol decomposes on (1 × 1)Pt(110) the C–O bonds break at low temperature to yield water, methane, hydrogen, and adsorbed carbon. Yet, all of the steps, kinks, and atoms of special coordination present on (1 × 1)Pt(110) are also present on (2 × 1)Pt(110). These results imply that the active site for C–O bond scission in methanol consists of an ensemble of many atoms rather than a step, kink, or atom of special coordination.

INTRODUCTION

Methanol decomposition on Pt(111) has previously been examined by Sexton *et al.* (*1*), Lüth and co-workers (*2, 3*), Abbas and Madix (*4*), and Levis *et al.* (*12*). Sexton *et al.* found that on their Pt(111) sample, the C–O bond stays intact during the decomposition process; only CO and H are formed. However, Abbas and Madix (*4*) and Levis *et al.* (*12*) found that on their Pt(111) samples, a fraction of the C–O bonds in the methanol break to yield carbon-containing fragments. On a clean sample, the carbon-containing fragments decompose upon heating to yield carbon (*4*). However, the carbon-containing fragments can be hydrogenated to methane in the presence of adsorbed sulfur. A small amount of methane formation is also observed during methanol decomposition on polycrystalline platinum (*5*).

Methanol decomposition has also been examined on Pd(111). Guo *et al.* (*17*) found that their Pd(111) sample will not dissociate the C–O bond in methanol. However, Levis *et al.* (*18*) observe C–O bond scission.

At present, no one knows why some investigators observe C–O bond scission while others do not. However, one possibility is that the bond dissociation process occurs on some special sites and the concentration of the special sites is different on the samples used by the different previous investigators. The objective of the work reported here was to see if there are sites on (1 × 1)Pt(110) which are especially active for the scission of the carbon–oxygen bond in methanol. This question arose because in recent work (*7, 8*) we have discovered that (1 × 1)Pt(110) is especially active for scission of the carbon–carbon single bonds in di-σ-ethylene. Based on our conception of the C–C bond scission process, the site for carbon–carbon bond scission should consist of a threefold fcc hollow site in one of the (111) terraces on the (1 × 1)Pt(110) surface and two C_7 atoms in the opposing step (see Fig. 1). Previous workers (*13–15*) have found that ethylene decomposes to μ_3-ethylidyne over the threefold fcc hollow sites on Pt(111). One might initially expect the threefold fcc hollow sites in (1 × 1)Pt(110) to behave similarly to the threefold hollow sites on Pt(111), and therefore catalyze

[1] To whom correspondence should be addressed.

0021-9517/90 $3.00

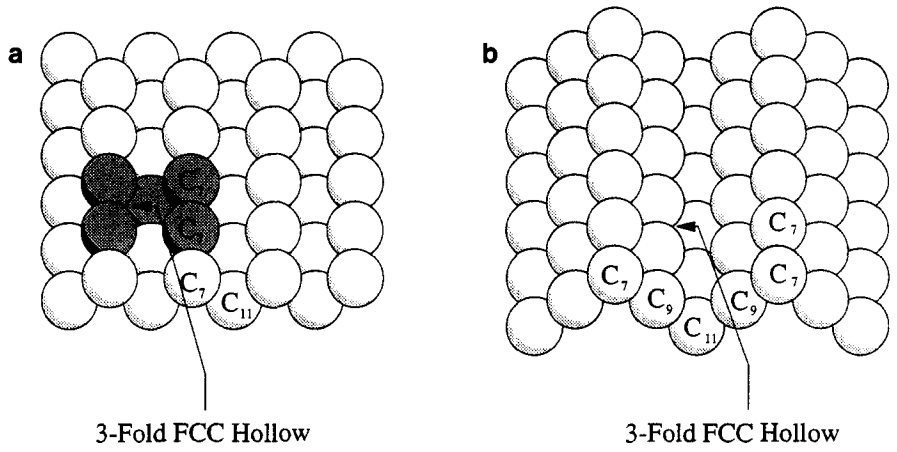

FIG. 1. Surface structures of (a) (1 × 1)Pt(110) and (b) (2 × 1)Pt(110). The active site for carbon–carbon bond scission proposed in Ref. (*7*) has been shaded in the figure.

ethylidyne formation. However, an unstrained ethylidyne cannot form on the (1 × 1)Pt(110) surface because the van der Waals radius of the methyl group in the ethylidyne would overlap the van der Waals radius of a C_7 atom in the (1 × 1)Pt(110) surface as illustrated in Fig. 2a. The ethylidyne would fit if the carbon–carbon bond stretched by about 0.5 Å as illustrated in Fig. 2b. Thus, there is a driving force for carbon–carbon bond extension on (1 × 1)Pt(110). Once the carbon–carbon bond stretches, it is then in a position to overlap orbitals on the C_7 atoms which have the right symmetry to promote

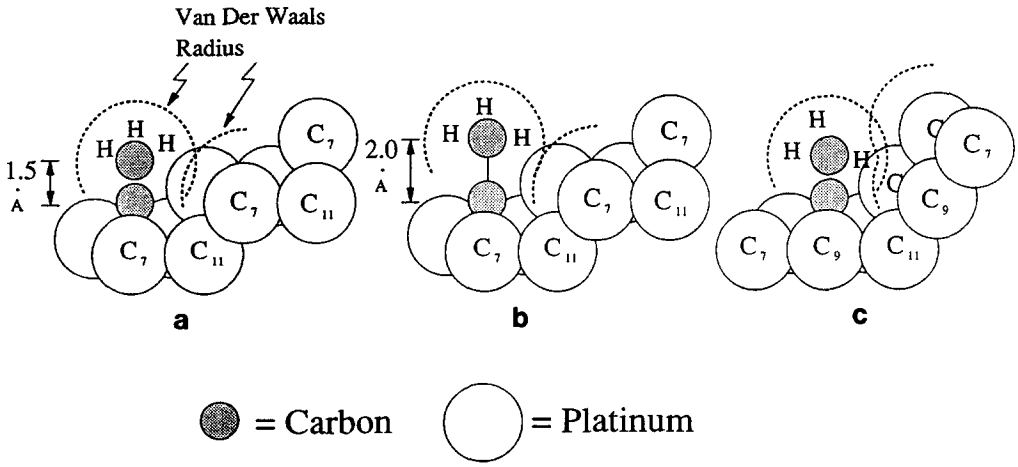

FIG. 2. (a) Geometry of an ethylidyne on (1 × 1)Pt(110) assuming that the ethylidyne forms over a threefold fcc hollow and the bond lengths and angles are the same as on Pt(111). Note that the van der Waals radius of the methyl group overlaps the van der Waals radius of the C_7 platinum atom. (b) A repeat of (a) assuming that the carbon–carbon bond length was expanded by 0.5 Å. Note that the van der Waals radii no longer overlap. (c) Geometry of an ethylidyne on (2 × 1)Pt(110) assuming that the ethylidyne forms over a threefold fcc hollow and the bond lengths and angles are the same as on Pt(111). Again the van der Waals radii overlap. However, in contrast to the results on (1 × 1)Pt(110), on (2 × 1)Pt(110) the C_7 atom blocks carbon/carbon bond extension. (a) Reproduced, with permission, from Ref.(*7*).

carbon–carbon bond scission. We believe that the combination of a favorable geometry for bond extension combined with the orbitals to promote bond scission makes carbon–carbon bond scission a favorable process on (1 × 1)Pt(110).

Carbon–carbon bond scission is much less favorable on (2 × 1)Pt(110) because the ethylidyne cannot simultaneously overlap the threefold fcc sites and the C_7 atoms.

Note that an argument analogous to the argument in the last two paragraphs might also be able to be applied to scission of the carbon–oxygen bond in methanol. Methanol's geometry is similar to that of ethylidyne. Previous data have shown that when methanol adsorbs on Pt(111) a strong bond forms between the two lone pair orbitals on the methanol and the (111) surface (*1, 2*). Details of the bonding are not understood. However, by analogy to the previous data, methanol might prefer to bind to the (111) terraces on (1 × 1)Pt(110). However, the methanol does not fit onto the terraces because the opposing step gets in the way. It happens that if the carbon–oxygen bond in methanol stretched everything would fit. Thus, there should be a driving force for carbon–oxygen bond extension on (1 × 1)Pt(110).

Once the carbon–oxygen bond stretches, it is in a position to overlap *d* orbitals on the C_7 atoms in the (1 × 1)Pt(110) surface which have the right symmetry to break carbon–oxygen bonds. The combination of a favorable geometry for bond extension combined with the right orbitals for bond scission *could* create a favorable situation for carbon–oxygen bond scission on (1 × 1)Pt(110). No similar situation exists on (2 × 1)Pt(110) because the methanol cannot bind to the terraces and still reach the C_7 atoms necessary for bond scission.

The objective of the experiments reported here was to see if carbon–oxygen bond scission does occur during methanol decomposition on (1 × 1)Pt(110). In our experiment we adsorbed methanol onto (1 × 1)Pt(110) at low temperatures, and then used temperature-programmed desorption (TPD) to look for evidence of carbon–oxygen bond scission. We also examined methanol decomposition on (2 × 1)Pt(110) where no carbon–oxygen bond scission was expected. The result of this study is to identify an active site for the scission of carbon–oxygen bonds in alcohols.

EXPERIMENTAL

The experiments reported in this paper were done using the apparatus and procedures described previously (*7–9*). The UHV system was of standard design with a working base pressure of 1×10^{-10} Torr. The system was equipped with a PHI 4-161 sputter gun, a PHI 15-120 LEED/AES system, and a Balzers QMA 112 mass spectrometer.

A (2 × 1)Pt(110) surface was prepared as described in our previous work (*7–9*). A Pt(110) single-crystal sample was cut from a Metron single-crystal rod. The sample was polished with diamond paste and then mounted in the vacuum system. The sample was then oxidized, sputtered, and annealed until no impurities could be detected by AES and a sharp (2 × 1) LEED pattern was seen.

The (1 × 1)Pt(110) sample was prepared by starting with a clean (2 × 1) sample then converting it to a (1 × 1) reconstruction via a procedure similar to that of Ferrer and Bonzel (*10*). The sample was heated to 600 K and exposed to 1×10^{-7} Torr of CO and then slowly cooled to 250 K in 1×10^{-7} Torr of CO. This procedure produced a CO-covered Pt(110) sample with a well-developed (2 × 1)p1g1 LEED structure and relatively high intensity between the LEED spots. The CO was then pumped away and the sample was cooled to 100 K. The sample was then bombarded for 3 min with 100-V electrons at an average current of 3 mA/cm^2 to desorb the CO remaining on the surface. The sample temperature rose to 200–220 K during the electron bombardment process. A trace of some sort of carbonaceous deposit was left behind on the crystal at the end of the electron bombardment proce-

dure. This carbonaceous deposit was removed by exposing the sample to 1×10^{-7} Torr of hydrogen at 200 K for 4 min. Then the hydrogen was removed by bombarding the surface with electrons for another 40 s at 90–170 K. At the end of this treatment, the sample showed a sharp (1 × 1) LEED pattern with little intensity between the spots. The sample also appeared clean by AES. However, TPD and EELS revealed that there was still a small amount of residual CO, H_2, and adsorbed carbon on the surface. Occasionally, there was also some subsurface oxygen.

There was some concern that these small amounts of impurities might be responsible for some of the novel chemistry discussed below. As a result, we also created an "almost (2 × 1)Pt(110)" surface by preparing a (1 × 1)Pt(110) sample as above and then annealing to 400 or 500 to partially convert the sample back to a (2 × 1) reconstruction. The sample was unchanged upon annealing to 300 K. The sample still showed a (1 × 1) LEED pattern after a brief anneal at 400 K. However, the (1 × 1) pattern was no longer sharp. Half-order spots were quite visible upon annealing to 500 K for 2 min. However, the half-order spots were not as sharp as with the (2 × 1)Pt(110) sample.

During a TPD run, the sample was dosed with a measured amount of vacuum-distilled methanol through a capillary array. The sample was then rotated so it faced an opening in a shield over the mass spectrometer. The geometry was such that only the front face of the crystal was in line of sight with the mass spectrometer. Next, the sample was heated at a fixed rate of 14 K/s under computer control. Everything else was standard. One should refer to Backman (*11*) for more details.

RESULTS

Figure 3a shows a composite TPD spectrum taken by exposing a clean (2 × 1)Pt(110) sample to 1.16 Langmuirs of methanol and then heating at 14 K/s. There are methanol peaks at 130 and 215 K, a hydrogen peak at 290 K, a carbon monoxide peak at 485 K, a 28-amu peak at 145 K, and a broad carbon monoxide desorption between about 150 and 300 K. For future reference, there is no evidence for desorption of methane or water during methanol decomposition on (2 × 1)Pt(110).

Traces of formaldehyde production were also detected at high coverages. However, the formaldehyde may be an artifact since much more formaldehyde is observed when the chamber is backfilled with methanol.

Figure 4 shows a series of 32-amu (methanol) spectra taken by exposing a clean (2 × 1)Pt(110) sample to various amounts of methanol and then heating at 14 K/s. At low exposures there is a single methanol peak at 130 K. The peak grows with increasing exposure. However, the peak temperature does not change with exposure. At high exposures there is evidence for formation of a second methanol peak at about 215 K. The height of the 215 K peak was found to decrease substantially on a defected sample, and increase in the presence of hydrogen. In other work, (*19*) it was found that this peak is associated with recombination of methoxy and hydrogen to yield methanol.

Figure 4 also shows a series of 28-amu (carbon monoxide) spectra taken by exposing a clean (2 × 1)Pt(110) sample to various amounts of methanol and then heating at 14 K–s. At low exposures, all of the carbon monoxide desorbs in a single peak at 485 K. The 485 K peak grows with increasing methanol exposure. In addition, a sharp peak at 145 K and a broad peak between 150 and 300 K grow into the 28-amu spectrum at high coverages. From the data, it is unclear whether the 145 K peak is associated with carbon monoxide, or simply cracking of the methanol on the walls of our chamber. However, the CO broad peak is not simply methanol cracking, since insufficient methanol desorption is observed at those temperatures to account for the peak.

Finally, Fig. 4 shows a series of 2-amu (hydrogen) spectra taken by exposing a clean (2 × 1)Pt(110) sample to various

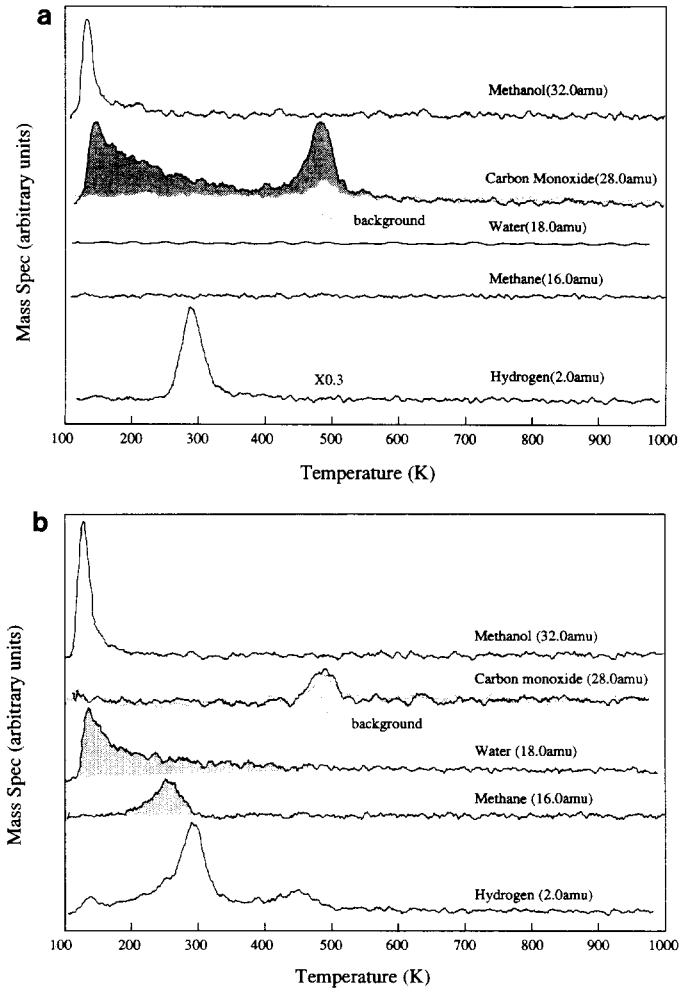

FIG. 3. Composite TPD spectrum taken by exposing a clean 93 K (a) (2 × 1)Pt(110) or (b) (1 × 1)Pt(110) sample to 1.16 or 1 Langmuir of methanol, respectively, and then heating at 14 K/s. The shaded areas on the figures indicate the difference between the signal and the background.

amounts of methanol and then heating at 14 K/s. At low methanol exposures hydrogen desorbs in a single peak at 315 K. This peak grows with increasing methanol exposure. Simultaneously, the peak shifts from 315 to 285 K. No additional features are seen at moderate methanol coverages. However, when the sample is exposed to 5 Langmuirs or more of methanol, a 2-amu peak at 140 K is seen. This peak is probably associated with cracking of formaldehyde or methanol in the ionizer of the mass spectrometer.

Figure 3b shows a composite TPD spectrum taken by exposing a clean (1 × 1)Pt(110) sample to 1.16 Langmuirs of methanol and then heating at 14 K/s. It has been found that the sample is converted to a (1 × 1) reconstruction, and the hydrogen peak is attenuated by about a factor of 3. The CO peak also goes down by more than an order of magnitude. There is always some residual CO on the surface, because CO is used to prepare the (1 × 1)Pt(110) surface. However, the 28-amu peak from methanol decomposition on (1 × 1)Pt(110) is at most only slightly larger than the 28-amu peak

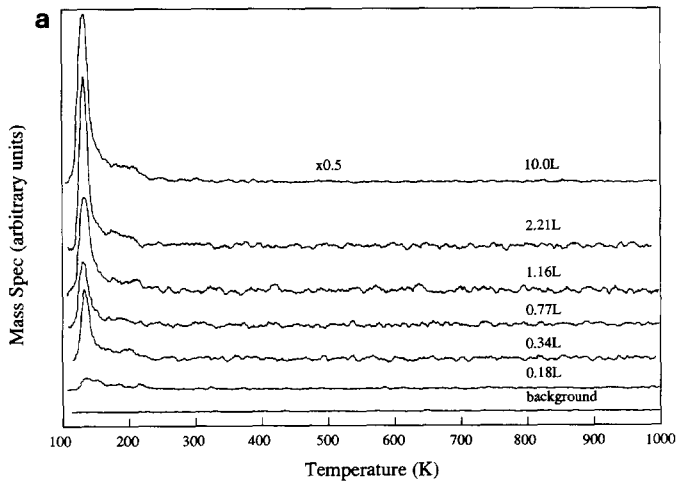

FIG. 4. Series of TPD spectra taken by exposing a clean 93 K (2 × 1)Pt(110) sample to varying amounts of methanol and then heating at 14 K/s. (a) 32 amu (methanol), (b) 28 amu (carbon monoxide), (c) 2 amu (hydrogen).

from the residual CO. The peak does not grow as the methanol exposure is increased above 0.1 Langmuir. Thus, we attribute the 28-amu peak observed during methanol decomposition on (1 × 1)Pt(110) to residual CO, and possibly some CO cracking on some imperfect regions of the sample. Therefore, we conclude that the production of CO is strongly suppressed and the Pt(110) surface is converted to a (1 × 1) reconstruction.

In the place of CO, we observe two new species during methanol decomposition on (1 × 1)Pt(110). We identify these species as methane and water. The species which we identify as water desorbs in a peak at 145 K and a tail extending up to 300 K. This species shows 18-, 17-, and 16-amu peaks in the ratio expected for water desorption. We do not observe any mass peaks in the tail except those expected for water. There could also be some small contribution at 17 and 18 amu from cracking of methanol in the mass spectrometer. However, at exposures of 2 Langmuirs or less, the expected contribution at 17 and 18 amu from methanol cracking is less than 2% of the 18-amu peak which is observed. We do not observe a significant 18-amu peak during methanol decomposition on (2 × 1)Pt(110) where no water forms (*6*). Hence, we assign the 18-amu peak shown in Fig. 3b to water which is produced during methanol decomposition on (1 × 1)Pt(110).

We assign the 250 K, 16-amu peak in Fig. 3b to methane. We have also measured spectra at 15 amu, and find that the 15- and 16-amu peaks at 250 K are in the right ratio for methane. There are no peaks at 250 K other than those expected for methane. Therefore, we assign the 16-amu peak in Fig. 3b to desorption of methane formed during methanol decomposition on (1 × 1)Pt(110).

Figure 5 shows a series of 32-amu (methanol) spectra taken by exposing a clean (1 × 1)Pt(110) sample to various amounts of methanol and then heating at 14 K/s. At low exposures there is a single methanol peak at 130 K which is similar to the methanol peak from (2 × 1)Pt(110). The peak grows with increasing exposure. However, the peak temperature does not change with exposure. Unlike the (2 × 1)Pt(110) case, there is no evidence for formation of a second methanol peak at high exposures.

Figure 5 shows also a series of 18-amu (water) spectra taken by exposing a clean (1 × 1)Pt(110) sample to various amounts of methanol and then heating at 14 K/s. At low

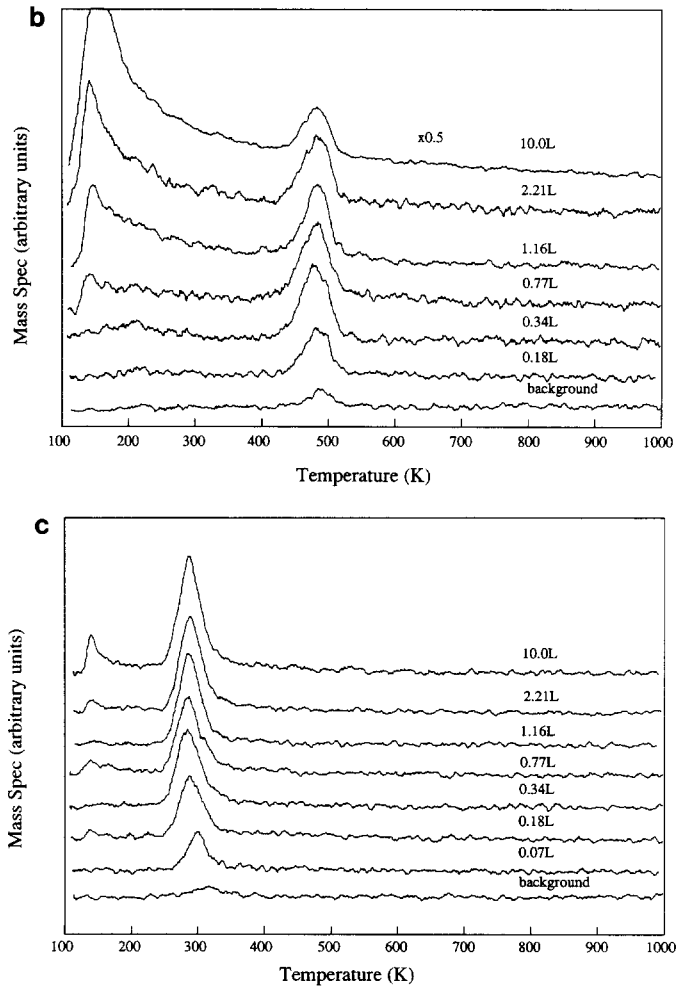

FIG. 4—*Continued*

exposures, a single water peak is seen at about 140 K. The water peak grows with increasing exposure. In addition, there appears to be a tail on the spectra which extends almost up to 300 K. The area of the peak continues to grow with increasing coverage even at high coverages because of a small contribution at 18 amu due to methanol cracking in the mass spectrometer. However, when we subtract that contribution away, we find that the water peak saturates at an exposure of 2–3 Langmuirs. We also observe a slight shift in the peak at a 10-Langmuir exposure. We attribute this shift to a small contribution at 18 amu due to methanol cracking in the ionizer of the mass spectrometer.

Figure 5 also shows a series of 16-amu (methane) spectra taken by exposing a clean (1 × 1)Pt(110) sample to various amounts of methanol and then heating at 14 K/s. At low exposures, a single small methane peak is seen at 260 K. The peak grows with increasing exposures. Simultaneously, the peak shifts to 245 K. At the highest exposures shown, there is also a small 16-amu peak at 140 K. This peak appears to be associated with cracking of methanol and water in the ionizer of the mass spectrometer.

Finally, Fig. 5 shows a series of 2-amu

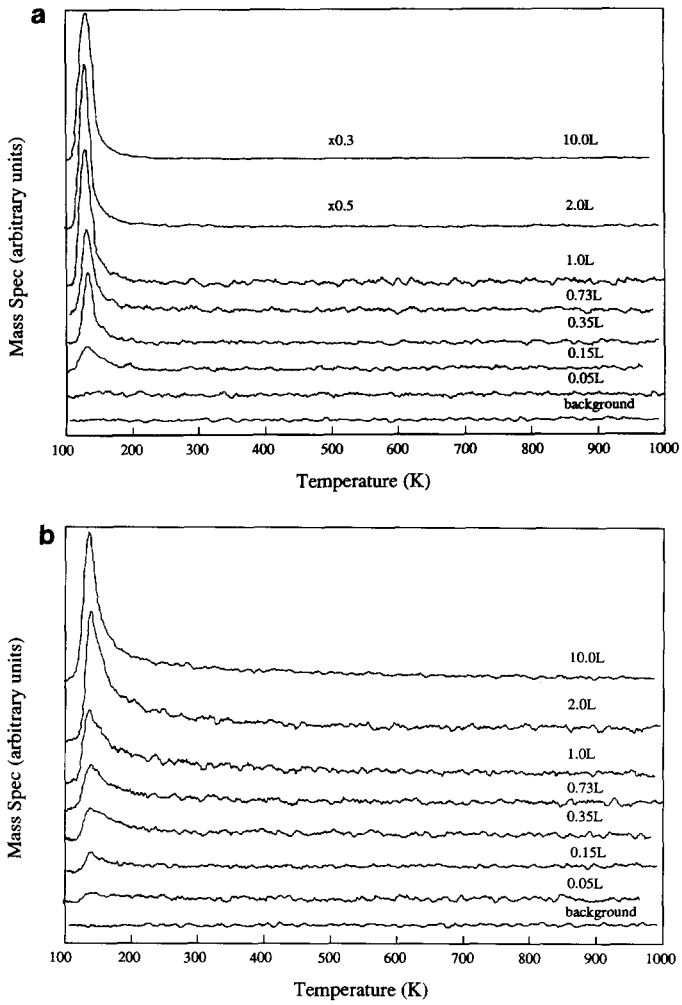

FIG. 5. Series of TPD specra taken by exposing a clean 93 K (1 × 1)Pt(110) sample to varying amounts of methanol and then heating at 14 K—s. (a) 32 amu (methanol), (b) 18 amu (water), (c) 16 amu (methane), (d) 2 amu (hydrogen).

(hydrogen) spectra taken by exposing a clean (1 × 1)Pt(110) sample to various amounts of methanol and then heating at 14 K/s. At low methanol exposures hydrogen desorbs in a single peak at 285 K and a smaller peak at 450 K. Both peaks grow with increasing methanol exposure. However, their peak positions are constant. At the highest exposure shown, we also observe a 2-amu peak at 130 K. Our interpretation of the data is that this peak is associated mainly with cracking of methanol in the ionizer of the mass spectrometer.

We have not included any CO spectra in Fig. 5. We did measure them. However, we did not observe any growth or changes of the CO peak with increasing methanol exposure. This provides further evidence that the small CO peaks observed during methanol decomposition on (1 × 1)Pt(110) in Fig. 3b are associated with either residual CO from our reconstruction procedure or some small amount of methanol decomposition on imperfect regions of the (1 × 1)Pt(110) surface.

We have also done Auger electron spectroscopy (AES) at the end of the TPD runs

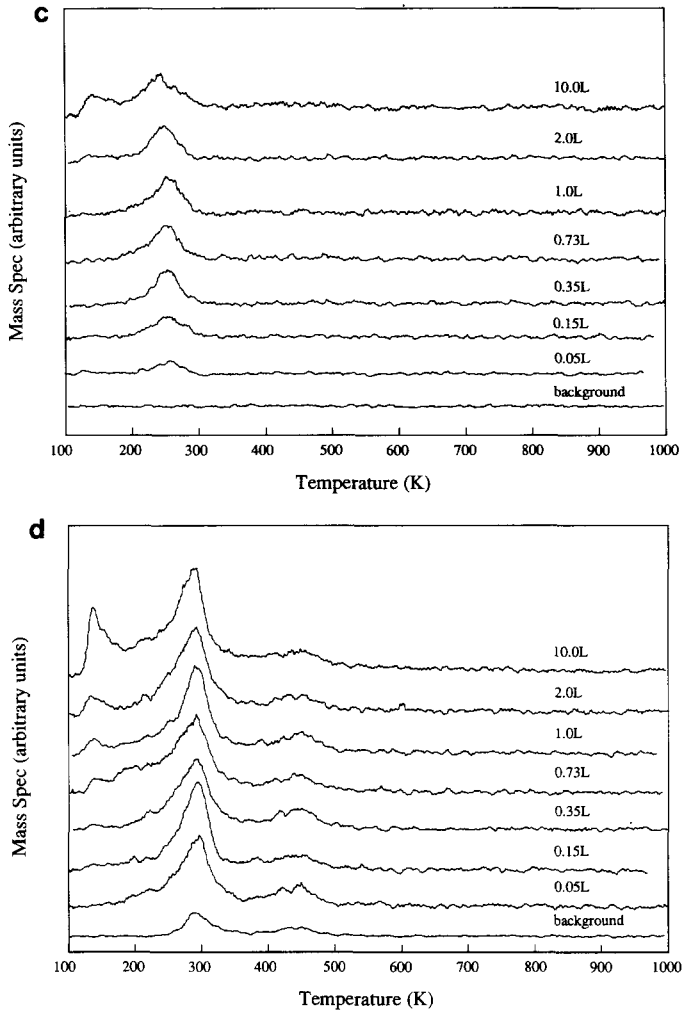

FIG. 5—*Continued*

used to obtain the data above. We find that on (1 × 1)Pt(110) there is a significant amount of carbon on the surface at the end of the TPD run. It is hard to be too quantitative with the AES data. However, it appears that over half of the carbon present in the ad-layer at 140 K remains on the surface at the end of a flash.

Finally, Fig. 6 shows a series of TPD spectra taken by preparing a (1 × 1)Pt(110) sample with deuterium rather than hydrogen, adsorbing 0.7 monolayer (2.21 Langmuirs) of methanol, 10 Langmuirs of deuterium, and then heating at 14 K/s. We observe peaks at 130 K corresponding to water (H_2O) and monodeuterated water (HDO) desorption, and a second group of peaks at 240 K corresponding to desorption of CH_4, CH_3D, CH_2D_2, CHD_3, and CD_4. Note, however, that the 19-amu peak from deuterated water is more than an order of magnitude smaller than the 18-amu peak from undeuterated water. As a result, we suggest that the water product is not substantially deuterated when we coadsorb methanol and deuterium. In contrast the methane product is clearly deuterated. We observe large peaks at 240 K in the 16-, 17-, and 18-amu

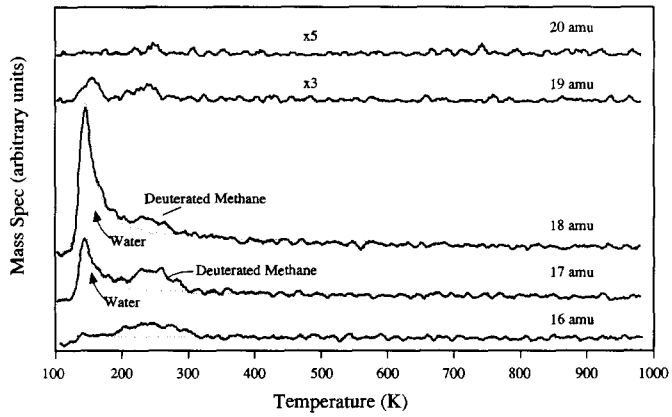

FIG. 6. Solid lines: series of TPD spectra taken by preparing a (1 × 1)Pt(110) sample with deuterium rather than hydrogen, exposing the surface to 2.21 Langmuirs of methanol then 10 Langmuirs of deuterium, and heating at 14 K/s. Dotted lines: three copies of an 18-amu (water) spectrum measured in the absence of deuterium. The height of the 18-amu spectrum has been adjusted to match the height of the water peak at 17 and 16 amu.

TPD spectra. The peak areas vary in the 1 : 1.7 : 1 ratio. The presence of the large 18-amu peak at 240 K implies that we are certainly producing CH_2D_2. The 17-amu peak is harder to interpret, since it contains contributions from both CH_2D_2 and CD_3D, we conclude that we are also producing some CH_3D. The 16-amu peak is even more difficult to interpret. It happens that if we add up the expected contribution at 16 amu from CH_2D_2 and CH_3D, we can account for the whole 16-amu peak. Thus, it is unclear whether any CH_4 forms. Certainly CH_4 is not a major reaction product. Hence, we suggest that when we react methanol and deuterium on (1 × 1)Pt(110) the main carbon- and oxygen-containing products are CH_2D_2, CH_3D, and H_2O.

DISCUSSION

The results above show that methanol decomposition on (1 × 1)Pt(110) is much different than that on any face of platinum studied previously (*1–6*). Previous work has shown that on Pt(111) the methanol decomposes exclusively to CO and H_2. There are also some TPD (*20*) and molecular beam data (*6*) which show that the methanol decomposes to CO and H_2 on (2 × 1)Pt(110). We confirm the previous results that methanol decomposes to CO and H_2 on (2 × 1)Pt(110). However, we are not able to detect significant CO desorption above our background levels on our (1 × 1) sample even though CO is the largest peak from our (2 × 1)Pt(110) sample. Instead we find that on (1 × 1)Pt(110) the carbon–oxygen bond breaks and the main products are hydrogen, methane, and water. Previous workers (*4, 5*) have found that small amounts of methane and water are formed on defected samples and polycrystalline platinum wires. However, at high coverages methane and water are the main decomposition products only on (1 × 1)Pt(110). Thus, it appears that (1 × 1)Pt(110) is unusually active for scission of the C–O bond in methanol; (2 × 1)Pt(110) shows no unusual activity, however.

The large difference in behavior of (1 × 1) and (2 × 1)Pt(110) is quite remarkable. We only have one sample. Yet when we pretreat the sample so that it shows a (2 × 1) LEED pattern, we get markedly different results than when we pretreat the sample so that it shows a (1 × 1) LEED pattern.

One obvious question is whether the differences in activity we observe are really associated with a change in surface structure. To address this issue, we tried an annealing experiment, where we prepared a (1

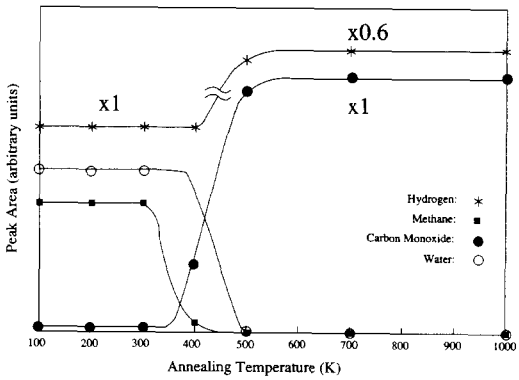

FIG. 7. Area of the carbon monoxide, hydrogen, methane, and water peaks measured by preparing a (1 × 1)Pt(110) surface as described in the experimental section, annealing to the temperatures indicated, cooling to 93 K, exposing the sample to 1.16 Langmuirs of methanol, and then heating at 14 K/s. The CO data were calculated from the area of the 28-amu peak with no connections for formaldehyde cracking in the mass spectrometer. Thus, the CO areas on the (2 × 1) structure may be slightly too large.

× 1)Pt(110) sample as above, annealed the surface to various temperatures to partially convert the sample back to a (2 × 1) reconstruction, and then adsorbed methanol and examined the decomposition process with TPD. Figure 7 shows how the area of the carbon monoxide, hydrogen, methane, and water peaks changed during this procedure. We find that when we anneal to 300 K the surface still shows a sharp (1 × 1) LEED pattern. The TPD spectrum of methanol from the annealed surface is identical to the TPD spectrum of methanol from the unannealed surface. In contrast, when we anneal the surface to 4–500 K, we start to see half-order spots characteristic of a (2 × 1) reconstruction. The methane and water peaks disappear at those temperatures, while the carbon monoxide and hydrogen peaks grow substantially. Note that in Fig. 6 we have multiplied the areas of the hydrogen peaks by 0.6 in the data obtained at annealing temperatures of 500 K or higher to keep the curves on the same scale. Thus, we find that the carbon–oxygen bond scission process we observe on (1 × 1)Pt(110) disappears as soon as we start to convert the surface to a (2 × 1) reconstruction. Therefore, we conclude that the unusual C–O bond scission activity noted above occurs on the (1 × 1) but not the (2 × 1) reconstruction of Pt(110).

It is interesting to consider the implications of the large difference in catalytic activity of (1 × 1)Pt(110) and (2 × 1)Pt(110). Most previous investigators associate active sites with steps, kinks, or atoms of special coordination. Note, however, that (1 × 1)Pt(110) and (2 × 1)Pt(110) have a very similar surface structure (see Fig. 1). Both surfaces are composed of (111) terraces and (111) steps. All of the steps, kinks, and C_x sites present on (1 × 1)Pt(110) are also present on (2 × 1)Pt(110). Thus, one would not have expected (2 × 1)Pt(110) to show markedly different catalytic activity than (1 × 1)Pt(110) based on the density of steps, kinks, or atoms of special coordination on the two surfaces. It is remarkable, therefore, that methanol decomposition on (1 × 1)Pt(110) is so much different than methanol decomposition on (2 × 1)Pt(110).

Of course, in our previous paper (7) it was argued that carbon–carbon bond scission requires a critical ensemble involving a threefold fcc hollow site and two C_7 atoms which lie close to it. The trends in the data here are quite similar to those in Ref. (7). We observe a large difference between the behavior of (1 × 1)Pt(110) and that of (2 × 1)Pt(110). The dropoff with annealing is identical to the one observed previously during ethylene decomposition on Pt(110). Therefore, the active site for carbon–oxygen bond scission must be similar for the two reactions. We suggest that the active site must involve a critical ensemble of platinum atoms rather than a step, kink, or atom of special coordination, since large differences in rate are observed during annealing, even though the step density is changing by only a factor of 2.

The details of this critical ensemble are not completely clear from the data here. Figure 8 shows two likely possibilities. If we limit our discussion to sites which are pres-

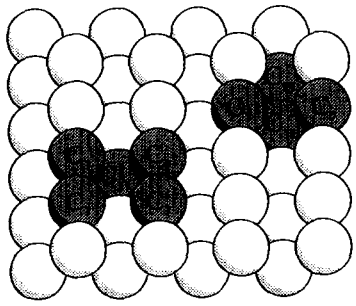

FIG. 8. Some of the likely active sites for C–O bond scission on (1 × 1)Pt(110).

ent on (1 × 1)Pt(110) but not on (2 × 1)Pt(110), we find that the active site must include at least a terrace site, and a C_7 atom on the opposing step. The size of the methanol is such that it would overlap at least four surface atoms, and perhaps five. Thus, the active site must include at least four atoms as in the shaded site on the right in Fig. 8, or five atoms as in the shaded site on the left. The active site could be larger than four or five atoms, however.

We need to do more work before we will be able to tell whether the active site is as small as the shaded sites in Fig. 8, or whether the active site includes additional atoms. It is also unclear whether there are sites on other faces of platinum which are also especially active for C–O bond scission. However, the data here show clearly that a critical ensemble of platinum atoms is needed to break the C–O bond in methanol. The active site is clearly not a step, kink, or atom of special coordination.

Before we close, we want to point out one expected feature in the data, the results of the deuterium, methanol coadsorption experiments in Fig. 6. In our previous experiments, we found that the carbon–carbon bond in ethylidyne broke on (1 × 1)Pt(110) to yield adsorbed methyl groups ($CH_{3(ad)}$) and adsorbed carbon ($C_{(ad)}$). The adsorbed methyl groups could then react with surface hydrogen to yield methane. We were expecting the same thing to happen during methanol decomposition on the (1 × 1) surface; i.e., the C–O bond should break to yield adsorbed hydroxyl groups ($OH_{(ad)}$) and adsorbed methyl groups. The adsorbed methyl and hydroxyl groups could then react with surface hydrogen to yield water and methane.

There are previous data (*12*) to indicate that adsorbed methyl groups could form during methanol decomposition on Pt(111) although the data are controversial (*17*). However, the results in Fig. 6 are not as we expected if OH's and CH_3's are forming during the reaction. Our experiments show that when we coadsorb methanol and deuterium, the oxygen leaves the surface as H_2O. Little HDO is observed. No D_2O or any other oxygen-containing products are detected. One can imagine the methanol breaking apart to CH_3's and OH's, and then the OH's reacting to form water via one of two pathways: a direct hydrogenation

$$OH + H_{(ad)} \rightarrow H_2O \qquad (1)$$

or a disproportionation

$$2OH \rightarrow H_2O + O_{(ac)} \qquad (2a)$$

$$O_{ad} + 2H_{(ad)} \rightarrow H_2O. \qquad (2b)$$

Note, however, that if reaction (1) occurred, a significant amount of HDO would form when methanol and deuterium are coadsorbed, whereas D_2O would be produced if reaction (2) occurred. Neither is observed even though we do deuterate a significant fraction of the methane desorption product. We also observe much more CH_2D_2 than one would expect if the methanol were decomposing to produce CH_3's. This seems to indicate that the methanol may be directly decomposing to CH_2's and H_2O and then the CH_2's are reacting to form methane, hydrogen, and adsorbed carbon. We cannot exclude a two-step mechanism for the formation of CH_2's, however:

$$CH_3OH_{(ad)} \rightarrow CH_3 + OH$$
$$\rightarrow CH_2 + H_2O. \qquad (3)$$

Details of this mechanism await further work.

CONCLUSION

In summary then, we find that methanol decomposition on (1 × 1)Pt(110) is far different than methanol decomposition on any face of platinum studied previously. While methanol decomposition on Pt(111) yields mainly CO and H_2, methanol decomposition on (1 × 1)Pt(110) yields mainly water, methane, hydrogen, and adsorbed carbon. In contrast, only CO and H_2 are detected on (2 × 1)Pt(110). Thus, it seems that there is an active site for C–O bond scission on (1 × 1)Pt(110). We postulate that the active site consists of a terrace site, which is closely aligned to a C_7 atom. However, confirmation that this is the active site for C–O bond scission requires further work.

ACKNOWLEDGMENTS

This work was supported by the National Science Foundation under Grant CTS 89-22282 and by Amoco Oil Company and Shell USA. Sample preparation was done using the facilities of the University of Illinois Center for Microanalysis of Materials, which is supported as a national facility, under National Science Foundation Grant DMR 89-20538. Equipment was provided by NSF Grants CPE 83-51648 and CBT 87-04667. Helpful discussions with Jay Benziger and Bob Madix are gratefully acknowledged.

REFERENCES

1. Sexton, B. A., *Surf. Sci.* **102,** 271 (1981). Sexton, B. A., Rendulic, D. D., and Hughes, A. E., *Surf. Sci.* **121,** 181 (1982).
2. Ehlers, D. H., Spitzer, A. P., Lüth, H., *Surf. Sci.* **160,** 57 (1985).
3. Ehlers, D. H., Esser, A., Spitzer, A. P., and Lüth, H., *Surf. Sci.* **191,** 466 (1987).
4. Abbas, N. M., and Madix, R. J., unpublished. Madix, R. J., personal communication (1990). See Abbas, N., Ph.D. dissertation, Stanford University, 1981.
5. Papapolymerou, G. A., and Schmidt, L. D., *Langmuir* **3,** 1098 (1987).
6. Gdowski, G. E., Fair, J. A., and Madix, R. J., *Surf. Sci.* **127,** 541 (1983).
7. Yagasaki, E., and Masel, R. I., *J. Amer. Chem. Soc.*, in press.
8. Yagasaki, E., and Masel, R. I., *Surf. Sci.* **222,** 430 (1989).
9. Yagasaki, E., Backman, A. L., and Masel, R. I., *J. Phys. Chem.* **94,** 1066 (1990).
10. Ferrer, S., and Bonzel, H. P., *Surf. Sci.* **119,** 234 (1982).
11. Backman, A. L., Ph.D. dissertation, University of Illinois, 1990.
12. Levis, R. J., Zhicheng, J., Winograd, N., Akhter, S., and White, J. M., *Catal. Lett.* **1,** 385 (1988).
13. Kesmodel, L. L., Dubois, L. H., and Somorjai, G. A., *J. Chem. Phys.* **70,** 2180 (1979).
14. Ibach, H., and Lewald, S., *J. Vac. Sci. Technol.* **15,** 407 (1978).
15. Skinner, P., Howard, M. W., Oxton, I. A., Kettle, S. F. A., Powell, D. B., and Sheppard, N., *J. Chem. Soc. Faraday Trans. 2* **77,** 1203 (1981).
16. Stenhagen, E., Abrahamsson, S., and McLafferty, F. W., "Atlas of Mass Spectral Data," Vol. 1, p. 2. Wiley, New York, 1969.
17. Guo, X., Hanley, L., and Yates, J. T., *J. Amer. Chem. Soc.* **111,** 3155 (1989).
18. Levis, R. J., Zhicheng, J., and Winograd, N., *J. Amer. Chem. Soc.* **110,** 4431 (1988).
19. Wang, J., Masel, R. I., unpublished.
20. Attard, G. A., Chibane, K., Ebert, H. D., and Parsons, R., *Surf. Sci.* **224,** 331 (1989).